energies

MDPI

Article

Modelling of Biomass Concentration, Multi-Wavelength Absorption and Discrimination Method for Seven Important Marine Microalgae Species

Jerónimo Chirivella-Martorell [1,†], Álvaro Briz-Redón [2,†] and Ángel Serrano-Aroca [3,*]

1 Institute of Environment and Marine Science Research (IMEDMAR), Universidad Católica de Valencia San Vicente Mártir, c/Guillem de Castro 94, Valencia 46001, Spain; jeronimo.chirivella@ucv.es
2 Departament d'Estadística i Investigació Operativa, Facultat de Matemàtiques, Universitat de València, c/Dr. Moliner, 50, Burjassot, València 46100, Spain; alvaro.briz@uv.es
3 Facultad de Veterinaria y Ciencias Experimentales, Universidad Católica de Valencia San Vicente Mártir, c/Guillem de Castro 94, Valencia 46001, Spain
* Correspondence: angel.serrano@ucv.es; Tel.: +34-963-637-412 (ext 5256)
† These two authors contribute equally to this paper.

Received: 26 March 2018; Accepted: 24 April 2018; Published: 28 April 2018

Abstract: Due to the possible depletion of fossil fuels in the near future and the necessity of finding new food sources for a growing world population, marine microalgae constitutes a very promising alternative resource, which can also contribute to carbon dioxide fixation. Thus, seven species (*Chaetoceros calcitrans*, *Chaetoceros gracilis*, *Isochrysis galbana*, *Nannochloropsis gaditana*, *Dunaliella salina*, *Tetraselmis suecica*, and *Tetraselmis chuii*) were grown in five serial batch cultures at a bench scale under continuous illumination. The batch cultures were inoculated with an aliquot that was extracted from a larger-scale culture in order to obtain growth data valid for the entire growth cycle with guaranteed reproducibility. Thus, measurements of optical density at several wavelengths and cell counting with a haemocytometer (Neubauer chamber) were performed every one or two days for 22 days in the five batch cultures of each specie. Modeling of cell growth, the relationship between optical density (OD) and cell concentration and the effect of wavelength on OD was performed. The results of this study showed the highest and lowest growth rate for *N. gaditana* and *T. suecica*, respectively. Furthermore, a simple and accurate discrimination method by performing direct single OD measurements of microalgae culture aliquots was developed and is already available for free on internet.

Keywords: modelling; culture; spectrophotometry; biomass concentration; marine microalgae; discrimination

1. Introduction

In the last decade, the great surge of interest in the microalgal world has been focused on the massive cultivation of microalgae for promising products, first and foremost among which has been microalgal fuel due to the possible depletion of fossil fuels in the near future and the idea of microalgae as a food source for a growing world population [1]. Marine microalgae constitutes a very promising biomass resource because their culture require neither available land nor freshwater [2,3]. Thus, there are microalgae species, such as the oleaginous *Nannochloropsis gaditana*, which has been proved to have high potential for biofuel production due to its high lipid content [4]. Novel processing technologies for the disintegration and extraction of microalgae to produce lipids and biofuels have been recently developed [5]. Furthermore, the fatty acid profile of algae can be significantly enhanced by the heterologous expression of exogenous genes [6] and using plant growth regulators [7].

Regarding the use of microalgae as a food source, the United Nations Advisory Committee has predicted a future extreme protein deficiency and encouraged researchers to work in this scientific field to avert hunger. In fact, a deficiency of 10 wt.% of polyunsaturated fatty acids (PUFA) is envisioned, and an increased in food prices is thus to be expected in fish meal without satisfying the world's growing demand [8]. Furthermore, microalgae culture can contribute simultaneously to both carbon dioxide fixation and wastewater treatment because they can be grown utilizing CO_2 from point sources such as power plants, cement manufacturing facilities and waste water from industrial, municipal, and dairy facilities [9,10].

On the other hand, marine microalgae constitute an almost exclusive live food for the larvae in the hatchery production of commercially valuable fish and shellfish. Among many microalgae that were identified for the aquaculture purposes, the genera of *Isochrysis* and *Chaetoceros* have extensively been used as food in most shrimp hatcheries in the last decades [11]. Microalgae species that were studied in this work, such as *Isochrysis galbana*, *Tetraselmis suecica*, and the diatoms *Chaetoceros calcitrans*, and *Chaetoceros gracilis* are widely cultured in applications of the bivalve aquaculture industry [12,13]. Diatoms are eukaryotic cells with cell walls containing very particular silica structures [8], which render these type of microalgae very promising for many applications, such as photonics, materials science, and nanotechnology [14].

In the last years, some microalgae species are gaining much attention in the marine drug research field for its high amount of Fucoxanthin [15] and other known and studied carotenoids, such as β-carotene from *Dunaliella salina* [16]. A number of studies have examined the metabolism, safety, and bioactivities of these carotenoids, including its anti-cancer, anti-obesity, antioxidant, anti-inflammatory, anti-diabetic, and anti-angiogenic activities [17,18].

One of the characteristics of microalgae is their different colours because each phylum usually has its own particular pattern of pigments and individual colour. However, some species, such as rhodophyta (red algae), can appear green (e.g., Mastocarpus stellatus) [19]. In view of their phylogenetic age, they have developed additional pigments that are unique to them [8]. It has been announced that the photosynthetic pigments and carotenoids that determine algal coloration are probably the constituents responsible for the antioxidant activity of this biomass source. However, the concentration of microalgal pigments may vary depending on the species and the activities of certain microalgae may also differ from one another [20]. Furthermore, other than antioxidant activity, it has been showed that some of the microalgae species that were studied in this work possess a biochemical content that would be very beneficial to humans and animals [8]. In fact, the European leading microalgae production company named *Fitoplancton marino S.L.* has recently achieved the European Novel Food approval for the marine microalgae species *Tetraselmis chuii* with excellent nutritional value and antioxidant activity [21]. In addition, most microalgae contain high levels of omega-3 polyunsaturated fatty acids (PUFA), omega-6 PUFA, and a high composition of essential amino acids [22].

Evaluating the cell growth cycle of algae is crucially important for algal applications [23]. In these studies, optical density (OD), also known as absorbance or turbidity, is frequently used as a rapid and non-destructive measurement of biomass in cultures of bacteria and other microorganism [24,25]. However, in the case of phytoplankton biomass, very significant inaccuracies can be introduced when the pigment content of the cells changes leading to significant errors in biomass quantification over the course of a growth cycle, due to the change in absorbance [26]. Nevertheless, algal density has been assessed by spectrophotometry for unicellular *Pseudokirchneriella subcapitata* [27] and other important species, such as *Chaetoceros calcitrans*, *Isochrysis affinis galbana* (T-Iso), *Nannochloropsis gaditana*, and *Phaeodactylum tricornutum* [28]. In these studies, the spectrophotometric equations were defined by choosing the wavelength producing maximum absorbance in order to determine cell density with maximum sensitivity. However, the purpose of the present study consisted of developing a multiple regression growth model that wsa based on direct OD measurements at different wavelengths of culture aliquots, which do not require performing any extraction procedure, and cell counting in a

haemocytometer for seven important marine microalgae species that were grown at bench scale under continuous illumination: *C. calcitrans*, *C. gracilis*, *I. galbana*, *N. gaditana*, *D. salina*, *T. suecica*, and *T. chuii*.

The use of a logistic function to represent cell growth over time has been proved to be successful in many studies during the last decades [29–31]. However, when the Gompertz model has been compared with the logistic function or other alternative models, such as the exponential or polynomial ones, it has been usually confirmed as a more flexible and accurate method to fit growth data [32]. For that reason, in this work, the Gompertz model was chosen to model the cell growth of the seven mentioned marine microalgae.

The development of a new accurate discrimination method, which is specifically designed for the identification and classification of microalgae, is very desirable for many bioengineering fields such as biofuel production, food industry, aquaculture, etc. In this research line, identification methods have been developed based on spectral fluorescence measurements [33] and microscopy image analysis [34,35]. However, absorbance data can also be utilised to design classification algorithms that are capable to discriminate between different microalgae species [36,37]. Thus, the last goal of the present study was focus on the development of a new prediction method for the recognition of these seven important marine microalgae species by means of a classification algorithm, which require direct OD measurements of culture aliquots (with no previous extraction) at any wavelength.

2. Materials and Methods

2.1. Microalgal Culture

Seven important marine microalgae species (*C. calcitrans*, *C. gracilis*, *I. galbana*, *N. gaditana*, *D. salina*, *T. suecica*, and *T. chuii*) were grown in 250 mL Erlenmeyer flasks in batch cultures using f/2 autoclaved medium [38] with a salinity of 35 g/L under continuous fluorescent illumination (6400 k cool white type; two tubes of 18 W) with a light intensity of 166.60 $\mu mol \cdot m^{-2} \cdot s^{-1}$ in a temperature controlled room at 27 ± 2 °C.

These marine microalgae species were obtained from the microalgae collection of the Institute of Environment and Marine Science Research at the Universidad Católica de Valencia San Vicente Mártir.

The carbon source was provided via bubbling of air enriched with 1% of CO_2 into the culture medium at a flow rate of 6.67 L/min.

Five serial 250 mL batch cultures were performed with each marine species. Thus, every day, during five days, 50 mL of inoculum were taken from a running 3 L fed-batch culture to be poured into a 250 mL Erlenmeyer flask. Subsequently, 200 mL of f/2 autoclaved medium was added to make the 250 mL of batch culture. The cultures utilised for the experiments were unialgal, but were non-axenic.

On the other hand, every day, 300 mL of fed-batch culture were harvested after taken the 50 mL of inoculum. Therefore, every day, 350 mL of fresh f/2 autoclaved medium had to be added to the fed-batch culture to keep it always with 3 L of microalgae culture in the exponential growth phase.

Every day, cell counting of the 3 L fed-batch culture was performed in order to check that the growth of this culture was kept in exponential phase during the five consecutive days.

The cellular density of the 3 L fed-batch culture and the five 250 mL batch cultures were determined by counting aliquots of cultures fixed with Lugol solution in a haemocytometer (Neubauer chamber) every one or two days until reaching the death cellular phase. Spectrophotometric measurements were performed in a Perkin Elmer lambda bio+ spectrophotometer. Thus, the direct spectrophotometric method followed in this work consisted of measuring optical density at several wavelengths that are similar to those used in the APHA method [39]. In this standard method, the optical density readings at 664, 647, and 630 nm are used to determine chlorophyll *a*, *b*, and *c*, respectively, and the absorption at 750 nm is a correction for turbidity. However, in this study, readings at more wavelengths were performed in order to have additional absorption values inside the absorption band of more types of pigments. Thus, OD measurements were performed at 480, 510, and 650 nm for carotenoid [40], fucoxanthin [41], and allophycocyanin [42] pigments, respectively.

However, to simplify the procedure, absorption measurements were performed directly in aliquots of cultures without carrying out any chemical extraction of pigments.

Some microalgae species tend to aggregate, especially the diatoms because their cell walls contain silica encased in an organic matrix [8]. Therefore, the culture aliquots of the seven microalgae species were homogenized with a vortex before OD measurements and cell counting.

2.2. Software

The R programming language (3.4.1 version, R Development Core Team, Vienna, Austria) [43] was utilised to perform the modelling and statistical analysis of the experimental results. Thus, the *ggplot2* (plot creation), *imputeTS* (time series missing values imputation), *nls* (non-linear model fitting), *nnet* (multi-class logistic regression fitting), *shiny* (app creation), and *TSClust* (time series dissimilarity distances computation) R packages were chosen for this work.

2.2.1. Growth Modelling

Cell concentration evolution was modelled using the Gompertz Equation (1) [44].

$$\sigma(t) = Ke^{-ae^{-rt}} \quad (1)$$

In this equation, the parameter K is the maximum value that is attainable by the function, r represents the growth rate of the curve, and a is the displacement along the x-axis.

The graphical representation of this equation is a characteristic sigmoid curve, which can model the entire cell growth cycle with the cell concentration that was obtained from the five serial 250 mL batch cultures (5 replicates) of each marine species. However, in this study, only the number of cells per mL during the lag and exponential phase were modelled as a function of time for each replicate of each microalgae species. The lag and exponential phase were determined as the period that comprises the beginning of the experiment and the maximum concentration of cells.

The *nls* (Nonlinear Least Squares) function of the R programming language [43] was utilised to perform the mathematical modelling [45]. Due to the fact that some of the available time series misses the measure of the concentration of cells for one or two days, an imputation process based on Kalman filtering was applied to the missing values before setting the model [46].

2.2.2. Relationship between OD Measurements and Cell Concentration

A multiple regression model was fitted to the observed concentration of cells per mL for the whole growth cycle (lag, exponential, stationary, and death phases) in order to obtain a global explanatory model of microalgae cell density at any time (days) of the cell growth cycle. The optical densities measured at the seven wavelengths and the type of microalgae was used as numerical covariates and as a factor respectively. The temporal variable was included in the form of a 4th degree polynomial to allow for the model to capture the underlying non-linear trend existing in a cell growth cycle.

2.2.3. Effect of the Wavelength on Optical Density

Consistency between OD measurements at the seven selected wavelengths (480, 510, 630, 647, 650, 664, and 750 nm) during the whole growth cycle was tested for all of the experiments. An imputation process that was based on Kalman filtering was also applied here at the missing values.

For all of the selected wavelengths, the Pearson correlation (ρ) between each combination of OD vs time series associated to each experiment was calculated. Assuming, x and y are two time series evaluated at n times, the Pearson correlation between x and y is computed in the following Equation (2).

$$\rho(x,y) = \frac{\sum_{i=1}^{n}(x_i - \overline{x})(y_i - \overline{y})}{\sqrt{\left(\sum_{i=1}^{n}(x_i - \overline{x})^2 \sum_{i=1}^{n}(y_i - \overline{y})^2\right)}} \quad (2)$$

Notice that the ρ value ranges from 0 (absence of correlation) to 1 (perfect correlation).

2.2.4. Microalgae Type Prediction from OD Measurements

A multi-class logistic regression model was defined to predict the seven probabilities of belonging an OD measurement to each of the seven microalgae studied.

In order to fit this prediction model for each of the OD measurements obtained, regardless of the type of microalgae, replicate, or wavelength, its average ρ value with the measurements belonging to each microalgae was computed for the five replicates and seven wavelengths.

Therefore, a multi-class logistic regression was fitted to the average ρ values between each OD measurement and type of microalgae with the function *multinom* of the R package *nnet* [47].

In addition to the ρ values, for purposes of comparison, two other important time series dissimilarity distances were used: Euclidean and dynamic time warping (DTW). The DTW distance can be implemented in the *TSClust* R package [48].

An R-*shiny* based web application [49] has been implemented to render possible the utilization of this algorithm to classify a specie of microalgae grown in similar conditions, as described in Section 2 of this study. The OD measurements used as input data should belong to a wavelength in the interval 480–750 nm, which correspond to the OD measurements employed to design the algorithm. However, the flexibility of the algorithm allows for the use of OD measurements at any wavelength. Moreover, the number of days of measurements should be as representative as possible to the microalgae growth cycle evolution.

The aforementioned application is allocated and is available for free on [50].

The only necessary input to run the application is a text file with columns to introduce the days of measurement and OD measurements. Once the text file is uploaded, the algorithm calculates the probability of belonging to each microalgae species for every introduced OD measurement introduced. After that, these results are shown on screen.

3. Results and Discussion

3.1. Growth Performance

The estimated average values of K, r and a, and the number of days after which the maximum concentration of cells was attained for the five replicates that were determined with the Gompertz Equation (1) are shown in Table 1. The width of a 90% confidence interval for these estimations, according to the five replicates, is also shown. Due to the small sample size, a 95th percentile of the *t-Student* distribution with four degrees of freedom was used.

Table 1. Estimated values of K, r, a, and the time in days to reach the maximum concentration of cells for the seven marine microalgae species that were determined with the Gompertz equation.

Species	K	r	a	Days
C. calcitrans	7,105,495 ± 102,350	0.39 ± 0.17	1.45 ± 0.32	6.0 ± 2.24
C. gracilis	3,403,165 ± 533,786	0.28 ± 0.08	1.58 ± 0.24	6.4 ± 1.09
I. galbana	14,033,908 ± 3,057,825	0.37 ± 0.18	2.01 ± 0.32	9.6 ± 1.98
T. suecica	1,781,854 ± 427,530	0.26 ± 0.15	1.69 ± 0.62	6.6 ± 2.49
T. chuii	1,980,891 ± 452,539	0.46 ± 0.41	2.55 ± 1.88	4.4 ± 0.52
D. salina	2,051,137 ± 433,004	0.41 ± 0.18	3.71 ± 1.29	5.8 ± 1.95
N. gaditana	17,729,210 ± 1,525,530	0.49 ± 0.16	1.49 ± 0.57	6.2 ± 1.71

Table 1 shows the fastest and slowest growth rate for *N. gaditana* and *S. suecica*, respectively (see their *r* values). This rapid growth of *N. gaditana* and the absolute lipid yield of *Nannochloropsis* strains, usually much higher than other marine microalgae [2], render this marine strain very promising specie for biofuel production at large scale in good agreement with a recent study [4].

The high growth rate of *T. chuii* (see its *r* value in Table 1), excellent nutritional value and demonstrated antioxidant activity [21], render this species very promising to be grown at large scale as a new food source necessary for the current growing world population. However, the low level of confidence that was determined with the Gompertz equation in this microalgae (see its *r* value) does not ensure a faster growth than the other six marine species. Furthermore, other mathematical models, such as the logistic function [30], were applied to the growth data of this species and showed similar results with a very wide confidence interval (results not shown).

The growth rate of *D. salina* was optimal at this laboratory conditions using a salinity of 3.5% (*w*/*v*), as expected [51], and has also been demonstrated to be a very suitable microalgae for biofuel production at large scale [52,53]. Table 1 shows that the Gompertz *a* value of *D. salina* was the highest, which can be attributed to a higher displacement along the *x*-axis, indicating that this species needed more time to start the exponential growth phase.

It can be observed how *I. galbana* required much more days to reach the maximum concentration of cells. However, *I. galbana* is widely used in aquaculture hatcheries because it grows faster than other species, such as *T. suecica* and *C. gracilis* (see their *r* values in Table 1) commonly utilised also in this nutritional field. *I. galbana* provides healthy growth for shellfish, because they are easy to maintain in large volume cultures, and produce significant amounts of PUFAS [54].

However, it is important to mention that all of these results were determined from experimental growth data obtained at bench scale under continuous illumination and thus cannot be directly extended to large-scale production.

Figure 1 shows the Gompertz curves of each marine microalgae species. These curves were obtained by averaging the Gompertz parameter estimates for the five replicates of each type of microalgae during the lag and exponential growth phases.

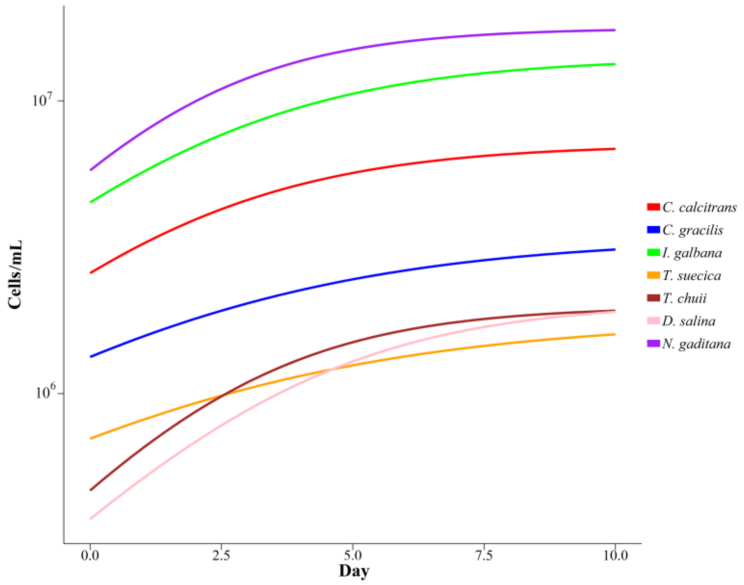

Figure 1. Gompertz fittings for the cellular growth of the indicated seven marine microalgae species during the lag and exponential growth phases. Curves obtained by averaging the Gompertz parameter estimates for the five replicates of each type of microalgae.

3.2. Explaining Cell Concentration from OD Measurements

The fitted multiple regression model showed a significant R^2 of 0.8748. The coefficients associated to each type of microalgae showed significance at the usual level (p-value < 0.05). Furthermore, the coefficients representing the polynomial effect of the number of days elapsed were all significant, and their estimates alternated their signs. Finally, and more interestingly, the absorbance at 480 nm appeared to be the only necessary OD measurement to model cell concentration. The high concordance that was showed by the absorbance at different wavelengths must have led to this fact.

When considering only the significant parameters of the model, a final explanatory Equation (3) can be determined.

$$\begin{aligned} Cells = &-2.594 \times 10^6\ C.\ calcitrans - 2.585 \times 10^6\ C.\ gracilis + 2.283 \times 10^6\ I.\ galbana \\ &- 2.599 \times 10^6\ T.\ suecica - 2.817 \times 10^6\ T.\ chuii - 2.341 \times 10^6\ D.\ salina + 3.698 \times 10^6\ N.\ gaditana \\ &+ 9.773 \times 10^5\ Day - 1.740 \times 10^5\ \mathrm{Day}^2 + 1.171 \times 10^4\ \mathrm{Day}^3 - 2.781 \times 10^2\ \mathrm{Day}^4 + 5.632 \times 10^5\ \mathrm{Abs}_{480} \end{aligned} \quad (3)$$

In this Equation (3), the names of the seven microalgae represent indicator variables, that is, variables with only two possible values: 0 or 1. In order to obtain the cell concentration estimation for a day in the growth cycle, it is necessary to choose 1 for the microalgae of interest and 0 for the rest of microalgae species.

Figure 2 includes the plots of the explanatory equations that fit the available data of the complete growth cycle for the seven marine microalgae species. The high level of smoothness for some of the curves indicates a robust and likely estimation of the whole growth cycle of the microalgae species. However, the more erratic curve estimated for *T. Suecica* could represent some lack of accuracy on the OD measurements for some of the experiments that were performed with this species.

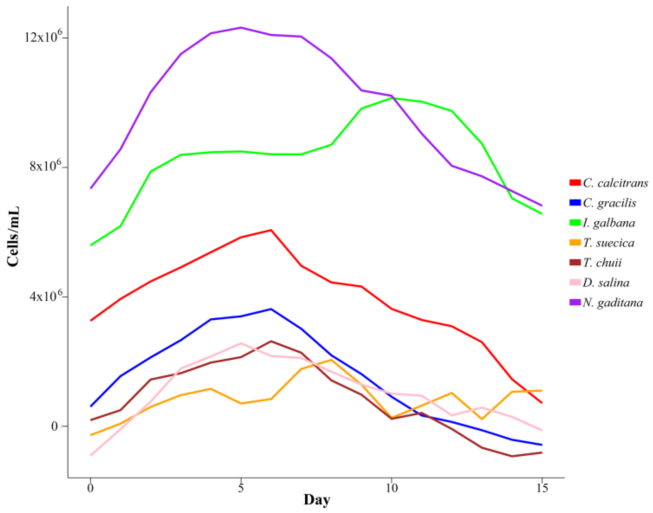

Figure 2. Cell growth for the indicated seven marine species based on the multiple regression equation.

It is of note that the extreme days of the growth cycle can show negative values in Figure 2 for some species, which should be taken into consideration if the model is employed with forecasting objectives.

Although the objective of fitting this model was only explanatory, it could also be utilised as a predictor of the evolution of biomass concentration as a function of time for the seven marine microalgae species that were grown in similar laboratory conditions.

3.3. Intra-Experiment OD Measurements

The average correlation values (ρ) for every different combination of wavelengths for each type of microalgae and replicate were computed. These values oscillated from 0.6 to 1, with a mean value of 0.95 and a standard deviation of 0.07, suggesting a very high agreement between the OD measurements

at different wavelengths. In fact, the highest average discrepancy between wavelengths showed a mean ρ value of 0.92 in the 35 experiments that were produced (Table 2).

These results support the consistency of the OD measurements because they showed very similar performance for most of the cultures regardless the selected wavelength.

Table 2. Correlation values (ρ) between optical density (OD) measurements at 480, 510, 630, 647, 650, 664, and 750 nm for all the performed experiments: five serial batch cultures of the seven marine microalgae species (35 correlations). Data shown as average ± standard deviation.

nm	480	510	630	647	650	664	750
480	1	0.96 ± 0.05	0.96 ± 0.06	0.95 ± 0.07	0.95 ± 0.07	0.94 ± 0.08	0.92 ± 0.09
510	0.96 ± 0.05	1	0.96 ± 0.07	0.95 ± 0.06	0.96 ± 0.05	0.95 ± 0.07	0.92 ± 0.08
630	0.96 ± 0.06	0.96 ± 0.07	1	0.96 ± 0.06	0.96 ± 0.06	0.97 ± 0.05	0.94 ± 0.08
647	0.95 ± 0.07	0.950.06	0.96 ± 0.06	1	0.96 ± 0.06	0.96 ± 0.05	0.95 ± 0.07
650	0.95 ± 0.06	0.96 ± 0.05	0.96 ± 0.06	0.96 ± 0.06	1	0.97 ± 0.06	0.94 ± 0.08
664	0.94 ± 0.08	0.95 ± 0.07	0.97 ± 0.05	0.96 ± 0.05	0.96 ± 0.06	1	0.95 ± 0.09
750	0.92 ± 0.09	0.92 ± 0.09	0.94 ± 0.08	0.95 ± 0.07	0.94 ± 0.08	0.95 ± 0.09	1

Table 3 shows the correlation values (ρ) between OD measurements at any of the seven selected wavelength for the five serial batch cultures (Replicates 1–5) of each marine microalgae species.

Table 3. Correlation values (ρ) between OD measurements at any wavelength (480, 510, 630, 647, 650, 664, and 750 nm) for each replicate of each marine microalgae species. Data shown as average ± standard deviation.

Species	Replicate 1	Replicate 2	Replicate 3	Replicate 4	Replicate 5
C. calcitrans	0.98 ± 0.02	0.99 ± 0.00	0.99 ± 0.00	0.99 ± 0.00	0.99 ± 0.00
C. gracilis	0.99 ± 0.00	0.99 ± 0.00	0.99 ± 0.00	0.99 ± 0.00	0.99 ± 0.00
I. galbana	0.99 ± 0.01	0.97 ± 0.04	0.99 ± 0.00	0.99 ± 0.00	0.99 ± 0.01
T. suecica	0.95 ± 0.03	0.89 ± 0.05	0.96 ± 0.02	0.92 ± 0.06	0.93 ± 0.04
T. chuii	0.89 ± 0.05	0.83 ± 0.06	0.86 ± 0.07	0.95 ± 0.04	0.92 ± 0.06
D. salina	0.91 ± 0.05	0.89 ± 0.09	0.93 ± 0.05	0.96 ± 0.02	0.93 ± 0.07
N. gaditana	0.98 ± 0.01	0.90 ± 0.13	0.91 ± 0.09	0.93 ± 0.09	0.91 ± 0.10

For example, Figure 3 represents the OD measurements as a function of time at the selected seven wavelengths (480, 510, 630, 647, 650, 664, and 750 nm) for the second batch culture of *T. chuii*. This culture showed the lowest average ρ between wavelengths (see Table 3).

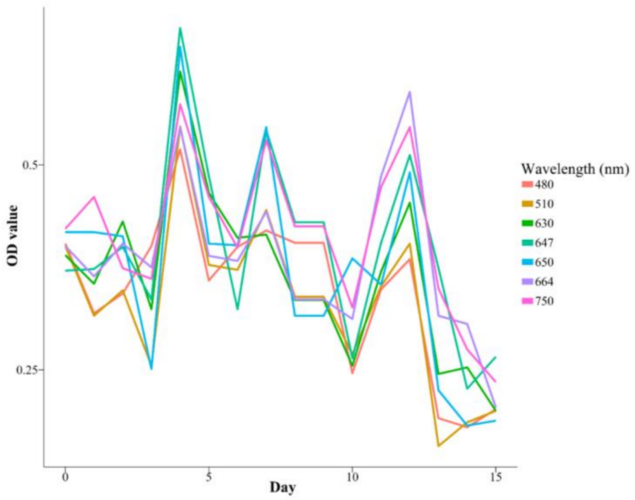

Figure 3. OD measurements as a function of time for the indicated seven wavelengths that were used in the second batch culture (Replicate 2) of the *Tetraselmis chuii* species.

However, some replicates, such as the first one of *I. galbana*, presented a ρ value that was very close to 1 for all of the wavelengths (see Figure 4 and Table 3).

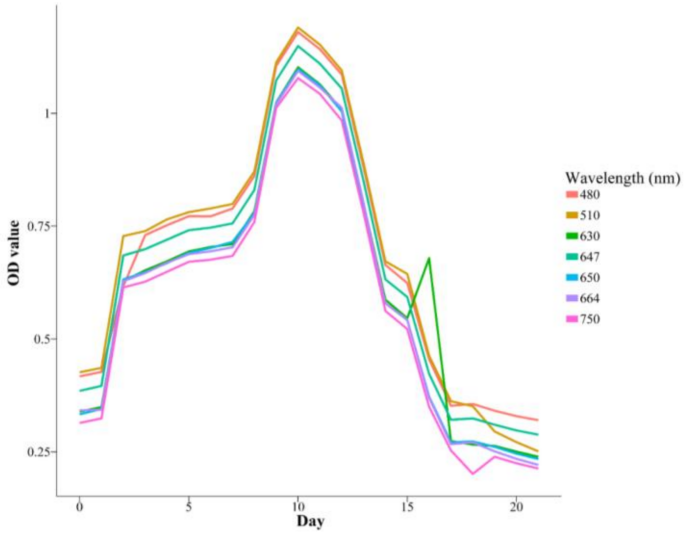

Figure 4. OD measurements as a function of time for the indicated seven wavelengths that were used in the first batch culture (Replicate 1) of the *Isochrysis galbana* species.

3.4. Inter-Experiment OD Measurements

The high level of robustness observed for the intra-experiment OD measurements at different wavelengths does not hold for some of the species when the correlations between OD measurements of the different experiments are checked for the same microalgae.

The correlation value is close to 1 for the OD measurements of *C. calcitrans* (0.98), *I. galbana* (0.97), and *C. gracilis* (0.86), regardless of the considered replicate and wavelength (see Table 4). The *D. salina* and *N. gaditana* species showed intermediate results, with a correlation value of 0.593 and 0.615. However, the level of agreement for *T. suecica* and *T. chuii* is far from good showing an inter-experiment correlation value below 0.5.

The high consistency for some of the species allows the establishment of groups of similar OD measurements, which correlate with the type of microalgae involved. This fact has been utilised in this work to define a classification algorithm for the seven marine microalgae species, whose performance is shown in the next section.

Table 4. Correlation values (ρ) between OD measurements of different replicates associated to the same microalgae specie, for each indicated wavelength. The last column includes the global correlation between OD measurements of different replicates of the corresponding microalgae species, regardless of wavelength. Data shown as average ± standard deviation (SD).

Species	480 nm	510 nm	630 nm	647 nm	650 nm	664 nm	750 nm	Mean ± SD
C. calcitrans	0.99 ± 0.01	0.96 ± 0.0	0.99 ± 0.01	0.99 ± 0.01	0.98 ± 0.01	0.98 ± 0.01	0.98 ± 0.01	0.98 ± 0.01
C. gracilis	0.84 ± 0.10	0.84 ± 0.10	0.84 ± 0.10	0.84 ± 0.10	0.83 ± 0.11	0.84 ± 0.09	0.84 ± 0.10	0.84 ± 0.09
I. galbana	0.97 ± 0.02	0.97 ± 0.03	0.96 ± 0.02	0.97 ± 0.02	0.97 ± 0.03	0.97 ± 0.02	0.96 ± 0.02	0.97 ± 0.02
T. suecica	0.15 ± 0.27	0.17 ± 0.30	0.17 ± 0.23	0.14 ± 0.32	0.15 ± 0.22	0.25 ± 0.21	0.21 ± 0.25	0.18 ± 0.21
T. chuii	0.44 ± 0.14	0.49 ± 0.15	0.46 ± 0.18	0.47 ± 0.15	0.40 ± 0.18	0.38 ± 0.27	0.47 ± 0.23	0.45 ± 0.27
D. salina	0.58 ± 0.17	0.61 ± 0.21	0.57 ± 0.23	0.61 ± 0.21	0.56 ± 0.16	0.60 ± 0.22	0.61 ± 0.17	0.59 ± 0.22
N. gaditana	0.65 ± 0.23	0.61 ± 0.23	0.65 ± 0.20	0.68 ± 0.20	0.66 ± 0.214	0.57 ± 0.19	0.48 ± 0.24	0.62 ± 0.19

3.5. Classification Algorithm Performance

The quality of the classifier was tested by *k*-fold cross-validation using a *k* value of 7. This implies the partition of the complete set of time series (a total of 245) in a train set of 210 series and a test set

of 35. The cross-validation process was repeated 1000 times, so that the estimated parameters could reach convergence.

Therefore, the classification algorithm was successful for all the species. Even though some of them presented higher error rate than the rest of the species. Table 5 contains the classification distribution (by rows) for each of the seven marine microalgae that were involved and the ρ method. The values in the diagonal entries also represent the level of sensitivity for each of the species.

Table 5. Distribution of values for the classification associated to each marine microalgae. Each row contains the percentage of cases that were assigned to each of the species for the microalgae OD measurements that the row represents.

Species	*C. calcitrans*	*C. gracilis*	*I. galbana*	*T. suecica*	*T. chuii*	*D. salina*	*N. gaditana*
C. calcitrans	97.43	2.57	-	-	-	-	-
C. gracilis	-	96.95	-	-	2.16	-	-
I.galbana	-	-	98.04	-	-	1.96	-
T. suecica	-	-	-	98.69	1.31	-	-
T. chuii	-	0.77	-	5.14	86.90	-	7.19
D. salina	-	-	-	-	1.70	97.28	1.02
N. gaditana	-	2.91	-	3.44	6.47	0.63	86.54

Table 5 shows that *T. chuii* and *N. gaditana* presented more cases of misclassification than the rest of the species. Thus, most of the times, *T. chuii* was predicted instead of *N. gaditana* or the opposite, and the misclassification of these two species as *T. suecica* also occurred.

These results are even outperformed by the Euclidean method and DTW with an average correct classification rate of 99.21 and 96.60, respectively.

Despite the excellent performance of the algorithm, it is important to mention that the OD measurements must be taken at similar growing conditions to those that are reported in this paper in order to keep its predictive capacity as much as possible.

This prediction method is very useful because it only needs to use a simple spectrophotometer to perform single direct OD measurements of culture aliquots, without the need of performing any chemical extraction procedure, at any wavelength. Therefore, it is very simple in comparison with other more complex methods developed by other authors, which require previous extraction and fluorescence spectra [36] or sophisticated equipment to obtain Fourier Transform InfraRed (FTIR) data [37].

4. Conclusions

Seven marine microalgae species (*C. calcitrans*. *C. gracilis*. *I. galbana*. *N. gaditana*. *D. salina*. *T. suecica*, and *T. chuii*) were grown at bench scale under continuous illumination from a larger-scale fed-up culture in exponential phase in order to measure optical density at several wavelengths (480, 510, 630, 647, 650, 664, 750 nm) and cell counting (cells·mL^{-1}) every one or two days for 22 days in five serial batch cultures of each specie. The results of this study showed the highest and lowest growth rate for *N. gaditana* and *T. suecica*, respectively, through the Gompertz mathematical modelling. A specific study about the effect of wavelength choice on OD measurements and the relationship between OD measurements and cell concentration was performed. Thus, a very high agreement was found between the OD measurements corresponding to the same experiment, downplaying the importance of the wavelength choice when only one replication is being considered. However, the lack of coherence appeared for some of the species. Finally, the high level of agreement found between the OD measurements of different replicates for some of the microalgae has led to the construction of an accurate microalgae classification algorithm that is able to discriminate microalgae by performing direct single OD measurements of culture aliquots.

The results of this study can be of great interest when the studied strains are intensively cultivated at larger scale under solar illumination for applications, such as biofuel, food, or feed production.

However, it is important to mention that these results have been obtained at bench scale under continuous illumination and thus cannot be directly extended to large scale.

Author Contributions: Ángel Serrano-Aroca and Jerónimo Chirivella-Martorell conceived the idea of this work. Álvaro Briz-Redón performed the mathematical analysis of this work and contributed to the manuscript text and figures. Jerónimo Chirivella-Martorell performed the marine microalgae culture experiments. Ángel Serrano-Aroca designed and supervised all the work, analysed and discussed the data results, and prepared the manuscript.

Acknowledgments: This work was supported by the PRUCV 2017-162-001. PRUCV 2017-231-001. PRUCV2018-162-001 and PRUCV2018-231-001 grants from the Universidad Católica de Valencia San Vicente Mártir.

Conflicts of Interest: The authors declare no conflict of interest.

References

1. Odjadjare, E.C.; Mutanda, T.; Olaniran, A.O. Potential biotechnological application of microalgae: A critical review. *Crit. Rev. Biotechnol.* **2015**, *37*, 37–52. [CrossRef] [PubMed]
2. Doan, T.T.Y.; Sivaloganathan, B.; Obbard, J.P. Screening of marine microalgae for biodiesel feedstock. *Biomass Bioenergy* **2011**, *35*, 2534–2544. [CrossRef]
3. Mata, T.M.; Martins, A.A.; Caetano, N.S. Microalgae for biodiesel production and other applications: A review. *Renew. Sustain. Energy Rev.* **2010**, *14*, 217–232. [CrossRef]
4. Sung, M.-G.; Lee, B.; Kim, C.W.; Nam, K.; Chang, Y.K. Enhancement of lipid productivity by adopting multi-stage continuous cultivation strategy in *Nannochloropsis gaditana*. *Bioresour. Technol.* **2017**, *229*, 20–25. [CrossRef] [PubMed]
5. Kröger, M.; Klemm, M.; Nelles, M. Hydrothermal Disintegration and Extraction of Different Microalgae Species. *Energies* **2018**, *11*, 450. [CrossRef]
6. Chen, G.; Chen, J.; He, Q.; Zhang, Y.; Peng, Z.; Fan, Z.; Bian, F.; Yu, J.; Qin, S. Functional Expression of the Arachis hypogaea L. Acyl-ACP Thioesterases AhFatA and AhFatB Enhances Fatty Acid Production in *Synechocystis* sp. PCC6803. *Energies* **2017**, *10*, 2093. [CrossRef]
7. Du, H.; Ahmed, F.; Lin, B.; Li, Z.; Huang, Y.; Sun, G.; Ding, H.; Wang, C.; Meng, C.; Gao, Z. The effects of plant growth regulators on cell growth, protein, carotenoid, PUFAs and lipid production of chlorella pyrenoidosa ZF strain. *Energies* **2017**, *10*, 1696. [CrossRef]
8. Richmond, A.; Hu, Q. *Handbook of Microalgal Culture: Applied Phycology and Biotechnology*, 2nd ed.; Wiley-Blackwell: Oxford, UK, 2013.
9. Razzak, S.A.; Ali, S.A.M.; Hossain, M.M.; DeLasa, H. Biological CO_2 fixation with production of microalgae in wastewater—A review. *Renew. Sustain. Energy Rev.* **2017**, *76*, 379–390. [CrossRef]
10. Lage, S.; Gojkovic, Z.; Funk, C.; Gentili, F. Algal Biomass from Wastewater and Flue Gases as a Source of Bioenergy. *Energies* **2018**, *11*, 664. [CrossRef]
11. Smith, L.L.; Fox, J.M.; Treece, G.D. Intensive algal culture techniques. In *Handbook of Mariculture Techniques, Crustacean Aquaculture*; CRC Press: Boca Raton, FL, USA, 1993.
12. Toro, J.E. The growth rate of two species of microalgae used in shellfish hatcheries cultured under two light regimes. *Aquac. Res.* **1989**, *20*, 249–254. [CrossRef]
13. Helm, M.M.; Bourne, N. *Hatchery Culture of Bivalves: A Practical Manual. FAO Fisheries and Aquaculture Department*; Food and Agriculture Organization of the United Nations: Rome, Italy, 2004.
14. De Angelis, R.; Melino, S.; Prosposito, P.; Casalboni, M.; Lamastra, F.R.; Nanni, F.; Bruno, L.; Congestri, R. The diatom Staurosirella pinnata for photoactive material production. *PLoS ONE* **2016**, *11*, e0165571. [CrossRef] [PubMed]
15. Kim, S.M.; Kang, S.W.; Kwon, O.N.; Chung, D.; Pan, C.H. Fucoxanthin as a major carotenoid in Isochrysis aff. galbana: Characterization of extraction for commercial application. *J. Korean Soc. Appl. Biol. Chem.* **2012**, *55*, 477–483. [CrossRef]
16. Raposo, M.F.; De Morais, A.M.; De Morais, R.M. Carotenoids from marine microalgae: A valuable natural source for the prevention of chronic diseases. *Mar. Drugs* **2015**, *13*, 5128–5155. [CrossRef] [PubMed]
17. Miyashita, K.; Nishikawa, S.; Beppu, F.; Tsukui, T.; Abe, M.; Hosokawa, M. The allenic carotenoid fucoxanthin, a novel marine nutraceutical from brown seaweeds. *J. Sci. Food Agric.* **2011**, *91*, 1166–1174. [CrossRef] [PubMed]

18. Helmersson, J.; Arnlöv, J.; Larsson, A.; Basu, S. Low dietary intake of beta-carotene, alpha-tocopherol and ascorbic acid is associated with increased inflammatory and oxidative stress status in a Swedish cohort. *Br. J. Nutr.* **2009**, *101*, 1775–1782. [CrossRef] [PubMed]
19. Blanco-Pascual, N.; Gómez-Guillén, M.C.; Montero, M.P. Integral *Mastocarpus stellatus* use for antioxidant edible film development. *Food Hydrocoll.* **2014**, *40*, 128–137. [CrossRef]
20. Metting, B.; Pyne, J.W. Biologically active compounds from microalgae. *Enzym. Microb. Technol.* **1986**, *8*, 386–394. [CrossRef]
21. Widowati, I.; Zainuri, M.; Kusumaningrum, H.P.; Susilowati, R.; Hardivillier, Y.; Leignel, V.; Bourgougnon, N.; Mouget, J.-L. Antioxidant activity of three microalgae *Dunaliella salina*, *Tetraselmis chuii* and *Isochrysis galbana* clone Tahiti This. *J. Phys. Conf. Ser.* **2017**, *55*, 012067. [CrossRef]
22. Natrah, F.M.I.; Yusoff, F.M.; Shariff, M.; Abas, F.; Mariana, N.S. Screening of Malaysian indigenous microalgae for antioxidant properties and nutritional value. *J. Appl. Phycol.* **2007**, *19*, 711–718. [CrossRef]
23. Takahashi, T. Toshiyuki Life Cycle Analysis of Endosymbiotic Algae in an Endosymbiotic Situation with Paramecium bursaria Using Capillary Flow Cytometry. *Energies* **2017**, *10*, 1413. [CrossRef]
24. Toennies, G.; Gallant, D.L. The relation between photometric turbidity and bacterial concentration. *Growth* **1949**, *13*, 7–20. [PubMed]
25. Lee, C.; Lim, H. New device for continuously monitoring the optical density of concentrated microbial cultures. *Biotechnol. Bioeng.* **1980**, *22*, 639–642. [CrossRef]
26. Griffiths, M.J.; Garcin, C.; van Hille, R.P.; Harrison, S.T.L. Interference by pigment in the estimation of microalgal biomass concentration by optical density. *J. Microbiol. Methods* **2011**, *85*, 119–123. [CrossRef] [PubMed]
27. Rodrigues, L.H.R.; Arenzon, A.; Raya-Rodriguez, M.T.; Fontoura, N.F. Algal density assessed by spectrophotometry: A calibration curve for the unicellular algae *Pseudokirchneriella subcapitata*. *J. Environ. Chem. Ecotoxicol.* **2011**, *3*, 225–228.
28. Santos-Ballardo, D.U.; Rossi, S.; Hernández, V.; Gómez, R.V.; del Carmen Rendón-Unceta, M.; Caro-Corrales, J.; Valdez-Ortiz, A. A simple spectrophotometric method for biomass measurement of important microalgae species in aquaculture. *Aquaculture* **2015**, *448*, 87–92. [CrossRef]
29. Pearl, R.; Slobodkin, L. The Growth of Populations. *Q. Rev. Biol.* **1976**, *51*, 6–24. [CrossRef]
30. Kacena, M.A.; Merrell, G.A.; Manfredi, B.; Smith, E.E.; Klaus, D.M.; Todd, P. Bacterial growth in space flight: Logistic growth curve parameters for Escherichia coli and Bacillus subtilis. *Appl. Microbiol. Biotechnol.* **1999**, *51*, 229–234. [CrossRef] [PubMed]
31. Chowdhury, B.R.; Chakraborty, R.; Chaudhuri, U.R. Validity of modified Gompertz and Logistic models in predicting cell growth of Pediococcus acidilactici H during the production of bacteriocin pediocin AcH. *J. Food Eng.* **2007**, *80*, 1171–1175. [CrossRef]
32. Zwietering, M.H.; Jongenburger, I.; Rombouts, F.M.; van 't Riet, K. Modeling of the bacterial growth curve. *Appl. Environ. Microbiol.* **1990**, *56*, 1875–1881. [PubMed]
33. MacIntyre, H.L.; Lawrenz, E.; Richardson, T.L. Taxonomic Discrimination of Phytoplankton by Spectral Fluorescence. In *Chlorophyll a Fluorescence in Aquatic Sciences: Methods and Applications*; Springer Netherlands: Dordrecht, The Netherlands, 2010; pp. 129–169.
34. Coltelli, P.; Barsanti, L.; Evangelista, V.; Frassanito, A.M.; Passarelli, V.; Gualtieri, P. Automatic and real time recognition of microalgae by means of pigment signature and shape. *Environ. Sci. Process. Impacts* **2013**, *15*, 1397–1410. [CrossRef] [PubMed]
35. Promdaen, S.; Wattuya, P.; Sanevas, N. Automated Microalgae Image Classification. *Procedia Comput. Sci.* **2014**, *29*, 1981–1992. [CrossRef]
36. Millie, D.F.; Schofield, O.M.E.; Kirkpatrick, G.J.; Johnsen, G.; Evens, T.J. Using absorbance and fluorescence spectra to discriminate microalgae. *Eur. J. Phycol.* **2002**, *37*, 313–322. [CrossRef]
37. Giordano, M.; Ratti, S.; Domenighini, A.; Vogt, F. Spectroscopic classification of 14 different microalga species: First steps towards spectroscopic measurement of phytoplankton biodiversity. *Plant Ecol. Divers.* **2009**, *2*, 155–164. [CrossRef]
38. Guillard, R.R.; Ryther, J.H. Studies of marine planktonic diatoms. I. *Cyclotella nana* Hustedt, and *Detonula confervacea* (Cleve) Gran. *Can. J. Microbiol.* **1962**, *8*, 229–239. [CrossRef] [PubMed]

39. Rice, E.W.; Baird, R.B.; Eaton, A.D.; Clesceri, L.S. (Eds.) *Standards Methods for the Examination of Water and Wastewater*, 22nd ed.; American Public Health Association, American Water Works Association, Water Environment Federation: Washington, DC, USA, 2016.
40. Sasaki, K.; Marquez, F.J.; Nishio, N.; Nagai, S. Promotive effect of 5-aminolevulinic acid on the growth and photosynthesis of Spirulina platensis. *J. Ferment. Bioeng.* **1995**, *79*, 453–457. [CrossRef]
41. Katoh, T.; Nagashima, U.; Mimuro, M. Fluorescence properties of the allenic carotenoid fucoxanthin: Implication for energy transfer in photosynthetic pigment systems. *Photosynth. Res.* **1991**, *27*, 221–226. [CrossRef] [PubMed]
42. Rakhimberdieva, M.G.; Vavilin, D.V.; Vermaas, W.F.J.; Elanskaya, I.V.; Karapetyan, N. V Phycobilin/chlorophyll excitation equilibration upon carotenoid-induced non-photochemical fluorescence quenching in phycobilisomes of the cyanobacterium *Synechocystis* sp. PCC 6803. *Biochim. Biophys. Acta* **2007**, *1767*, 757–765. [CrossRef] [PubMed]
43. Team, R.C. *R Language Definition*; R Foundation for Statistical Computing: Vienna, Austria, 2000.
44. Buchanan, R.L.; Whiting, R.C.; Damert, W.C. When is simple good enough: A comparison of the Gompertz, Baranyi, and three-phase linear models for fitting bacterial growth curves. *Food Microbiol.* **1997**, *14*, 313–326. [CrossRef]
45. Bates, D.M.; Watts, D.G. (Eds.) *Nonlinear Regression Analysis and Its Applications*; Wiley Series in Probability and Statistics; John Wiley & Sons, Inc.: Hoboken, NJ, USA, 1988.
46. Hyndman, R.J.; Khandakar, Y. Automatic time series forecasting: The forecast package for R. *J. Stat. Softw.* **2007**, *27*. [CrossRef]
47. Venables, W.N.; Ripley, B.D. *Modern Applied Statistics with S-PLUS*; Springer: New York, NY, USA, 1999; ISBN 9781475731217.
48. Montero, P.; Vilar, J.A.; Montero, P.; Vilar, J.A. TSclust: An R Package for Time Series Clustering. *J. Stat. Softw.* **2014**, *62*. [CrossRef]
49. Chang, W.; Cheng, J.; Allaire, J.J.; Xie, Y.; McPherson, J. Shiny: Web Application Framework for R. 2017. Available online: https://rdrr.io/cran/shiny/ (accessed on 27 April 2018).
50. Microalgae Classifier Based on Absorbance (Optical Density) Data. Available online: https://albriz.shinyapps.io/microalgaeclassification/ (accessed on 25 March 2018).
51. Al-Hasan, R.H.; Ghannoum, M.A.; Sallal, A.-K.; Abu-Elten, K.H.; Radwan, S.S. Correlative Changes of Growth, Pigmentation and Lipid Composition of *Dunaliella salina* in Response to Halostress. *Microbiology* **1987**, *133*, 2607–2616. [CrossRef]
52. Cho, K.; Lee, C.H.; Ko, K.; Lee, Y.J.; Kim, K.N.; Kim, M.K.; Chung, Y.H.; Kim, D.; Yeo, I.K.; Oda, T. Use of phenol-induced oxidative stress acclimation to stimulate cell growth and biodiesel production by the oceanic microalga *Dunaliella salina*. *Algal Res.* **2016**, *17*, 61–66. [CrossRef]
53. Cho, K.; Hur, S.P.; Lee, C.H.; Ko, K.; Lee, Y.J.; Kim, K.N.; Kim, M.S.; Chung, Y.H.; Kim, D.; Oda, T. Bioflocculation of the oceanic microalga *Dunaliella salina* by the bloom-forming dinoflagellate *Heterocapsa circularisquama*, and its effect on biodiesel properties of the biomass. *Bioresour. Technol.* **2016**, *202*, 257–261. [CrossRef] [PubMed]
54. Patil, V.; Källqvist, T.; Olsen, E.; Vogt, G.; Gislerød, H.R. Fatty acid composition of 12 microalgae for possible use in aquaculture feed. *Aquac. Int.* **2007**, *15*, 1–9. [CrossRef]